Geochemical Perspectives Letters EAG

Expanding Mars' lithologic diversity: discovery of a garnet-bearing clast in NWA 8171

T.V. Kizovski[1,2*], L.F. White[3], A. Černok[4], K.T. Tait[1,5], V.E. Di Cecco[1], X. Chu[5], J.M. Tomacic[1,5], R.I. Nicklin[1], J.R. Darling[6]

OPEN ACCESS
https://doi.org/10.7185/geochemlet.2619

Abstract

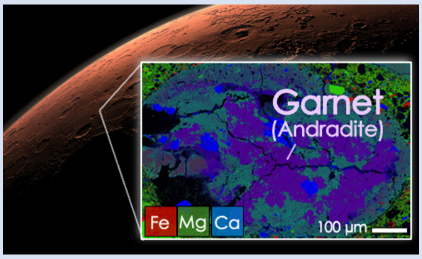

A garnet-bearing clast has been identified in martian breccia meteorite NWA 8171, comprising two distinct domains: an andradite-diopside domain, and a K-feldspar-augite domain. Similar assemblages occur in terrestrial metamorphic/metasomatic settings like skarns, in alkali igneous rocks; and as secondary phases in carbonaceous chondrites. Mineralogical and textural analyses of the clast reveals a complex history, possibly reflecting multiple crystallisation stages and/or alteration events on Mars. However, as NWA 8171 is a regolith breccia, we also consider if the garnet-bearing clast is extra-martian in origin. Analysis of pyroxene Mn/Fe ratios indicate that augites from the K-feldspar-rich domain match martian values, while diopsides in the andradite-bearing domain are more varied in composition. This variability, together with similarities to metasomatic assemblages from chondritic and terrestrial analogues, suggests that the andradite-rich domain may not comprise primary igneous minerals. This could indicate the clast was altered on Mars in an oxidising metasomatic event, although an extra-martian origin cannot be ruled out. Still, the first identification of garnet in a martian meteorite has major implications. The andradite-bearing clast in NWA 8171 may be the first sample of a garnet-bearing lithology from Mars, representing a previously unidentified martian magma source, alteration process, regolith impactor component, or metamorphic event.

Received 28 October 2025 | Accepted 17 April 2026 | Published 16 June 2026

Introduction

In order to define the geologic processes that shaped Mars over its 4.5 billion year history, characterising its mineral diversity is essential. At this time, only ~200 minerals are known or inferred to occur on Mars (Hazen *et al.*, 2023); significantly less than the ~6000 minerals on Earth (Hazen *et al.*, 2008). This contrast is mainly attributed to Mars' lack of plate tectonics, widespread water, and life – at least through most of its history (Hazen *et al.*, 2023). However, the large differences in mineral diversity between the two planets can also be ascribed to the lack of high resolution mineralogical data from Mars, with only ~400 martian meteorites and 10 martian landing sites explored *in situ* (Udry *et al.*, 2020). As minerals, and the rocks they make up, are products of complex interactions between the lithosphere, atmosphere, hydrosphere, and even biosphere; detailed analyses of newly discovered martian rocks and minerals are crucial for identifying previously unidentified geologic processes.

Here, we present the preliminary mineralogical and chemical characterisation of a garnet-bearing rock type in martian meteorite Northwest Africa (NWA) 8171 – the first identification of a garnet-bearing lithology from Mars.

NWA 8171. NWA 8171 is one of 18 martian regolith breccia meteorites, all paired to the same meteorite fall. They are classified as polymict breccias as they comprise a variety of clasts from several different source lithologies embedded in a fine-grained matrix (Agee *et al.*, 2013; Humayun *et al.*, 2013; McCubbin *et al.*, 2016; Hewins *et al.*, 2017). The clasts' source rocks are most likely from the ancient southern highlands of Mars, with some clasts estimated to be ~4.4 billion years old (Ga) (Humayun *et al.*, 2013). They were eventually assembled and lithified into a breccia during an impact event ~1.5 Ga (McCubbin *et al.*, 2016). Due to their polymict nature, there are significant heterogeneities between each of the paired stones, providing the opportunity to discover new martian rock types like the recently recognised granitic rock fragments in paired meteorite NWA 7533 (Malarewicz *et al.*, 2025) and the garnet-bearing rock in NWA 8171 described here. More information on NWA 8171 and paired meteorites is provided in the Supplementary Information (SI).

1. Department of Natural History, Royal Ontario Museum, Toronto, ON M5S 2C6, Canada
2. Department of Earth Sciences, Brock University, St. Catharines, ON L2S 3A1, Canada
3. Planetary and Space Sciences, School of Physical Sciences, The Open University, Milton Keynes MK7 6AA, United Kingdom
4. Dipartimento di Matematica, Informatica e Geoscienze, Universita di Trieste, 34128 Trieste, Italy
5. Department of Earth Sciences, University of Toronto, Toronto, ON M5S 3B1, Canada
6. Institute of the Earth and Environment, University of Portsmouth, Portsmouth PO1 3QL, United Kingdom
* Corresponding author: (email: tkizovski@brocku.ca)

Materials and Methods

One grain mount of NWA 8171 (ROMESM58935 from the Royal Ontario Museum) was analysed. No thin sections were available. Mineral compositions, chemical maps, bulk composition estimates, and backscatter electron (BSE) images were acquired using electron microprobe, and scanning electron microscopes. Electron backscattered diffraction (EBSD) maps of the clast, and Raman spectra for the major minerals were also collected. More details on these methods are provided in the SI.

Results

The garnet in NWA 8171 has been identified by Raman, EBSD, and microprobe as andradite ($Ca_3Fe^{3+}{}_2(SiO_4)_3$) occurring in a rounded clast (~540 μm × 830 μm) embedded in the meteorite's matrix (Fig. 1).

The clast comprises two textural and mineralogical domains: an andradite-rich domain with subhedral to anhedral andradites in a fine-grained diopside matrix, and a K-feldspar-rich (K-spar) domain of coarse-grained feldspar and augite. Chlorapatite is a significant component of both domains, and is distinctly euhedral in the K-spar-rich domain. Fine-grained intergrowths of diopside, andradite, grossular, and feldspar occur at the contact between the domains (Fig. 1e,g).

Andradite-rich domain. Microprobe analyses of the andradites indicate they are relatively homogenous ($Adr_{97}Grs_{2.1}Prp_{0.6}Sps_{0.3}$; mineral abbreviations in Table S-1), although some grains display zoning from Fe^{3+}-rich cores to Ca,Al-rich rims, as well as randomly distributed enrichments of Ca and Al ($Adr_{91.8}Grs_{7.4}Prp_{0.6}Sps_{0.2}$) (Fig. 1b, Table S-3). The andradite grains also exhibit embayed margins and contain numerous diopside inclusions. Although not detected by microprobe, EDS mapping reveals Al-rich regions at andradite/K-spar and andradite/clast-rim boundaries. Raman spectra from these regions are consistent with andradite and/or grossular, indicating an Al-rich ugrandite garnet is present. These regions were not analysed by microprobe due to their fine grain size (Figs. 1, S-8).

The diopside-rich matrix ($En_{39.2}Fs_{11.8}Wo_{49}$) exhibits patchy Fe enrichments ($En_{31.1}Fs_{20.2}Wo_{48.7}$), and also includes several Na-rich plagioclase grains ($Ab_{50.2–72.4}An_{48.2–21.5}Or_{1.6–6}$). EBSD analysis reveals good crystallinity in the plagioclase, but a significant portion of the diopside-rich matrix is amorphous at the scale of our analyses (1–0.35 μm step size; Fig. 2). Where crystalline, diopside grains are typically <5 μm in size (Fig. 2d). Microprobe analyses of the diopside indicate good pyroxene stoichiometry (pyroxene structural sites [T, M1, M2] all filled as expected; Table S-5) with analytical totals close to 100 % (Table S-3). Apatites in the andradite-rich domain are Cl-rich (3.54–4.55 wt. % Cl) with relatively high Si compositions (average $SiO_2 = 1.95 \pm 1.34$ (s.d.) wt. %; Table S-5). The high Si measurements are well correlated with lower totals and higher Mg concentrations, interpreted here as mixtures of chlorapatite and Mg-Si-rich inclusions (likely diopside; Fig. S-2). Apatite EBSD indicates that they are dominantly amorphous, containing sparse, randomly oriented <5 μm fragments of crystalline apatite (Fig. S-2). Due to the wide range of orientations, the apatite halogen abundances reported in Table S-5 should be regarded as qualitative estimates only, as F and Cl X-ray count rates have been shown to vary significantly during microprobe analyses of apatite, and are strongly dependent on crystal orientation (*e.g.*, Stormer *et al.*, 1993).

EDS and EBSD mapping illustrate compositional zoning in the fine-grained component of the andradite-rich domain (Figs. S-3, S-5), with an Mg-diopside-rich core; Mg-poor, Fe-Al-rich (garnet- and feldspar-rich) poorly crystalline inner rim; and thin Mg-rich outer rim (likely diopside) in contact with the breccia's clastic matrix. The fine-grained rim does not extend into the K-spar-rich domain. Fe-Ti oxides are also present in this rim, with trace anhedral 10–20 μm titanite grains (identified by EDS; Figs. 1f, S-4). These Ti-rich phases are also observed at the contact between the andradite-rich and K-spar-rich domains.

K-feldspar-rich domain. The K-spar-rich domain is dominated by Fe-rich augite and K-Na-rich feldspar. The augites exhibit zoning from relatively Fe-rich cores ($En_{21}Fs_{40}Wo_{39}$) to thin slightly Fe-poor rims ($En_{22}Fs_{37}Wo_{41}$), although this zoning is more pronounced in EDS maps (Fig. S-3). The feldspars also show evidence of zoning with K-rich rims, and patchy exsolution varying between $Ab_{31}An_6Or_{63}$ and $Ab_{57}An_7Or_{36}$ (Fig. 1d). Apatites in the K-rich domain are slightly more F-rich than those in the andradite-rich domain (average wt. % $F = 0.93 \pm 0.28$ (s.d.) and 0.71 ± 0.07 (s.d.), respectively). EBSD analyses show that the augite grains and the larger apatite grains in the K-spar-rich domain are strongly crystalline, while the feldspar grains are almost entirely amorphous at the scale of the analyses carried out here (1 μm step size; Fig. 2b). However, Raman analyses of the feldspars indicate some crystallinity with strong orthoclase peaks evident in several point measurements, and featureless spectra in others (Fig. 3a). The feldspars in the coarse domain also include numerous Fe, Mg, and Ti-rich inclusions (Fig. 1f), that may be contributing to the ~660 cm^{-1} peak in orthoclase Raman spectra (Fig. 3b). The K-rich feldspars also often exhibit slightly lower analytical totals in microprobe analyses (98.5 % on average; Table S-3). Al-enrichments associated with grossular-andradite and/or poorly-crystalline finely intergrown unidentified Ca-Fe-Al silicates with low analytical totals occur at boundaries between K-spars and the andradite-rich domain (Figs. 1, S-8, Table S-3).

Discussion and Conclusions

The first identification of a garnet-bearing rock type in a martian meteorite is significant. Notably, garnet is an important metamorphic mineral on Earth (Baxter *et al.*, 2017). Terrestrial andradite garnets are commonly associated with contact metamorphism and metasomatism, occurring with diopside-hedenbergite in skarns or rodingites (Li *et al.*, 2004; Chiama *et al.*, 2023). However, on Mars, the extent and nature of metamorphism remains speculative (McSween, 2015), limited to putative identifications of metamorphic phases in orbital spectra such as prehnite, chlorite, and epidote (Ehlmann *et al.*, 2011; Carter *et al.*, 2013), and rare *in situ* detections of serpentine likely formed by magmatic devolatisation (*i.e.* Tosca *et al.*, 2025).

Alternatively, andradite garnets can also crystallise in igneous settings. On Earth, assemblages of andradite, clinopyroxenes, and K-spar similar to those in NWA 8171, have been identified in alkaline igneous rocks (Chiama *et al.*, 2023). Extrusive alkali-rich rocks (trachytes and trachy-andesites) have been identified in martian meteorites and *in situ* on the martian surface (Payré *et al.*, 2024; Schmidt *et al.*, 2025). As no garnet has been identified in these rocks, if igneous, the garnet-bearing clast in NWA 8171 could represent a distinct stage of alkali-rich magma differentiation, and/or a previously unrepresented magma source.

Since andradite-bearing assemblages can form in a variety of geological environments, here we present a discussion of the possible origins for the garnet-bearing clast in NWA 8171, and the implications for Mars.

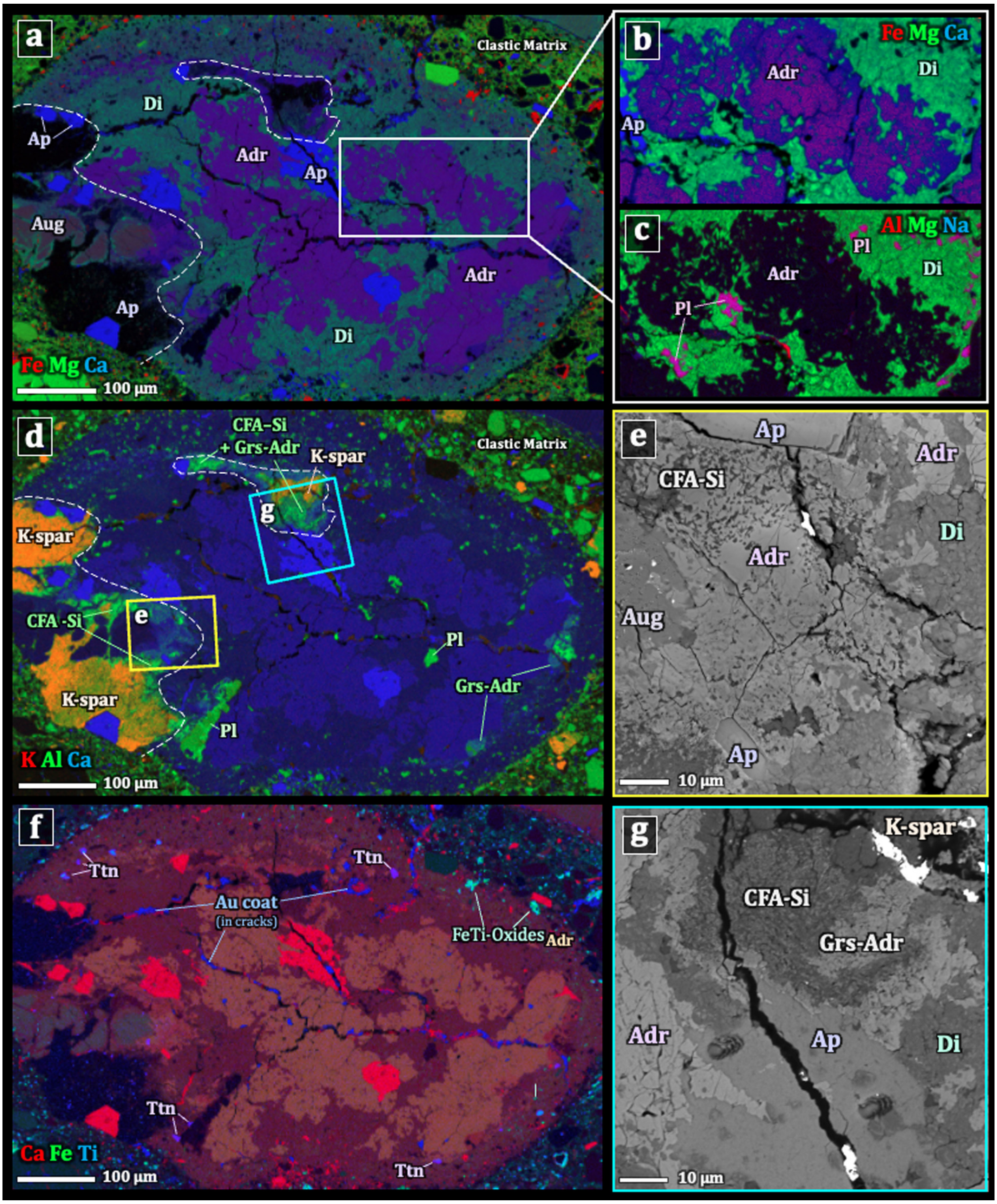

Figure 1 Chemical maps of the garnet-bearing clast. **(a)** Red-Green-Blue (RGB) map of Fe (R), Mg (G), and Ca (B) with the main phases labelled and the boundary between the domains delineated with white dashed lines. **(b)** RGB map of Fe (R) contrast stretched to show details, Mg (G), and Ca (B). **(c)** RGB map of Al (R), Mg (G), and Na (B). **(d)** RGB map of K (R), Al (G), Ca (B) highlighting feldspars, andradite-grossular and poorly crystalline unidentified Ca-Fe-Al-rich silicates (CFA-Si). **(e)** BSE image of the contact between the two domains showing irregular intergrowths of Ca-Fe-Al-rich silicates (CFA-Si) with andradite, augite, K-spar, and diopside. **(f)** RGB map of Ca (R), Fe (G), Ti (B) highlighting the Ti-rich phase occurrences. Some bright blue areas (Ti-rich) are remnant Au-coat in cracks from previous analyses. **(g)** BSE image of the domain contact area showing CFA-Si, grossular-andradite, diopside, K-spar, apatite, and andradite.

Potential origins of the garnet-bearing clast. Firstly, as NWA 8171 is a regolith breccia, it is necessary to consider if the garnet-bearing clast is extra-martian in origin, delivered and incorporated into regolith on the surface of Mars through impacts. While no physical non-martian components have been found in the martian regolith breccia meteorites, elevated siderophile concentrations in these meteorites indicate the incorporation of ~5 % CI chondritic material (*i.e.* Humayun *et al.*, 2013). In addition, numerous meteorites have been found on the surface of Mars by rovers, with 15 classified in the Meteoritical Bulletin (https://www.lpi.usra.edu/meteor/).

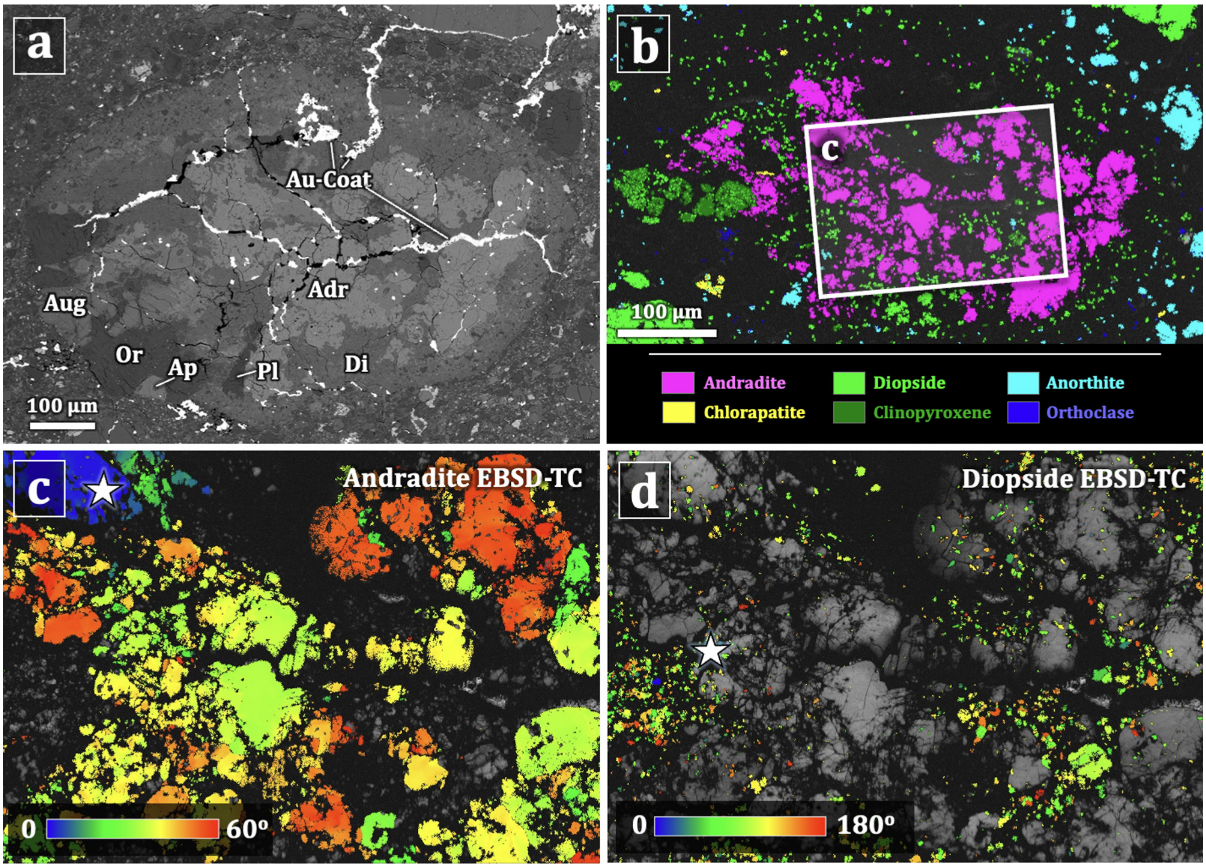

Figure 2 Electron backscatter diffraction (EBSD) of the garnet-bearing clast. **(a)** BSE image with the main phases labelled, including remnant Au-coat. **(b)** Phase map of the minerals identified by EBSD (1 µm step size). **(c, d)** Texture Component (TC) figures showing relative orientations of andradite **(c)** and diopside **(d)**. EBSD-TC maps display crystallographic mis-orientation relative to defined points of reference (white stars).

While the mineralogy of the garnet-bearing clast is not consistent with these meteorites, andradite-bearing assemblages have been identified as secondary metasomatic phases in several carbonaceous chondrites including oxidised CVs (Vigarano-like), COs (Ornans-like), and more rarely, CMs (Murchison-like) (MacPherson and Krot, 2014; Ganino and Libourel, 2020; Jenkins *et al.*, 2025). In these chondrites, andradite typically occurs with other Ca-Fe silicates within, or rimming Calcium Aluminum Inclusions (CAIs) and chondrules, but can also be found surrounding dark lithic inclusions, and/or disseminated in matrix material (Krot *et al.*, 1998a, 1998b; MacPherson and Krot, 2014; Ganino and Libourel, 2020). Chondritic andradite is most commonly associated with diopside-hedenbergite, wollastonite, and feldspathoids ± sulfides ± metal, with these assemblages occurring as pseudomorphs and replacements of Fe-rich minerals, in veins and cavities, and/or as nodules in the fine grained matrix (Krot *et al.*, 1998a, 1998b; MacPherson and Krot, 2014; Ganino and Libourel, 2020).

These assemblages are often finer grained than the garnet in NWA 8171, but there are some textural and compositional similarities; with subhedral andradite in CV chondrites often occurring in a fine grained matrix of Ca-Fe-Si-rich minerals (Fig. S-6). Pyroxene major element compositions are also very similar to chondrites (*i.e.* Fe, Mg, Ca; Fig. 4).

In order to further narrow down the origin of the garnet-bearing clast, we also examined pyroxene Mn/Fe ratios (Fig. 4), a commonly used geochemical marker for primary igneous pyroxenes from various planetary bodies (Papike *et al.*, 2009). As shown in Figure 4 and Figure S-7, the Mn/Fe ratios of the pyroxenes in the garnet-bearing clast generally fall in the same range as those from other paired martian breccias, although these values are often between Earth and Mars. The pyroxenes in the garnet-bearing domain however, show significant variation, extending into the compositional fields for chondrites, the Earth, Moon, and Vesta (Fig. 4). While the wide range of Mn/Fe ratios in the pyroxenes from the andradite-rich domain could indicate a different parent body, it could also indicate that this domain formed from secondary alteration processes on Mars. Lower Mn/Fe ratios are often associated with secondary oxidation on Mars (Yen *et al.*, 2010) and pyroxenes with elevated Mn/Fe ratios have been identified in clast-laden impact melt rocks in other paired breccia samples (Hewins *et al.*, 2017). The garnet-bearing domain is also intergrown with the K-spar-rich domain (Figs. 1, S-8), which contains augite with martian Mn/Fe ratios. However, Mn/Fe ratios of secondary pyroxenes in carbonaceous chondrites can also overlap with the martian compositional field (Fig. S-7); thus, although a martian origin is likely, Mn/Fe ratios alone cannot definitively rule out an extra-martian origin.

Regardless of its parent body, the clast's precise petrogenesis remains difficult to constrain. Given the small sample size, it is challenging to determine whether the two domains equilibrated under the same conditions. Feldspar thermometry from the K-spar-rich domain indicates a high crystallisation temperature of 900 to 1000 °C (Fig. S-9; after Benisek *et al.*, 2004). The patchy perthitic feldspars, large apatites, and Fe-rich augite with a lack of orthopyroxene in this domain are also somewhat similar to the igneous perthitic and monzonitic clasts in NWA 8171 pairs

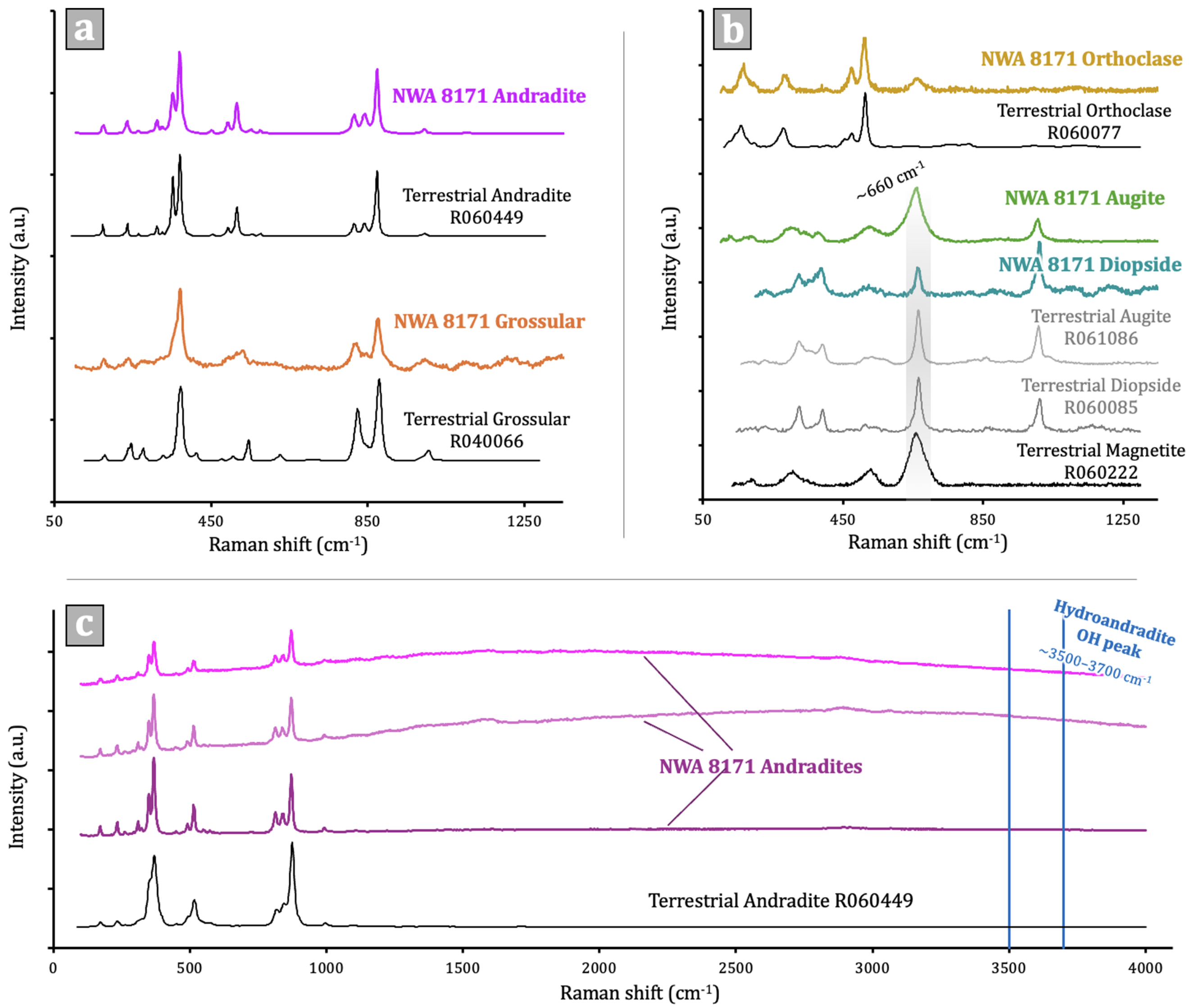

Figure 3 Raman spectroscopy of various minerals in the garnet-bearing clast. Spectra are normalised to 1 and offset for clarity. **(a)** Representative Raman spectra for garnet in NWA 8171, and **(b)** other major minerals, with comparisons to the RRUFF database (Lafuente *et al.*, 2016). Potential phases contributing to the ~660 cm^{-1} hump in orthoclase are also shown. **(c)** Raman spectra from 3 andradite point analyses showing the absence of a peak at ~3500–3700 cm^{-1} that is typical when hydroandradite ($Ca_3Fe^{3+}{}_2(SiO_4)_{3-x}(OH)_{4x}$) is present (*i.e.* Jenkins *et al.*, 2025).

(Hewins *et al.*, 2017; Figs. S-10 to S-12). The lack of plagioclase in the K-spar-rich domain, which is common in monzonitic clasts, could be due to sampling bias; or this domain could represent a previously unsampled syenitic lithology. However, Fe-rich augite is relatively rare in martian regolith breccias, and the perthitic exsolution observed here is more subtle in comparison (Fig. S-12).

The plagioclase in the andradite-rich domain implies a lower crystallisation temperature <900 °C (Fig. S-9), possibly reflecting later crystallisation or a subsequent alteration process. The lack of obvious hydro-andradite, minimal OH in apatite, and high analytical totals for andradite and diopside indicate that this assemblage formed in relatively anhydrous conditions (Fig. 3c, Table S-3). Secondary andradite-diopside assemblages in aqueously altered carbonaceous chondrites may likewise be anhydrous, likely because they formed at relatively low water/rock ratios (MacPherson and Krot, 2014).

The fine grained corona/rim surrounding the garnet-rich domain may have formed after the original rock was incorporated into the breccia. An impact event could have induced localised reactions and partial recrystallisation of this region through contact with the hot clastic matrix. In contrast, the K-rich domain, representing a higher temperature assemblage, may have been less reactive and therefore less susceptible to overprinting under these conditions.

If we use carbonaceous chondrites as an analogue, the andradite-bearing assemblage in NWA 8171 could have formed on the surface of Mars through localised, low temperature, fluid-assisted thermal metamorphism which dissolved Ca, Fe, Mg, and Si that eventually precipitated as the Ca-Fe-silicate assemblages (Krot *et al.*, 1998a, 1998b; MacPherson and Krot, 2014). This process may have replaced minerals within the K-spar-rich domain, with grossular-andradite forming at orthoclase interfaces and andradite + diopside at greater distances from these boundaries. However, the nearly end-member andradite compositions that dominate NWA 8171 are unusual, indicating extremely oxidising conditions.

Evidence for such oxidising environments on Mars is abundant. The martian regolith breccia meteorites are considered among the most oxidised martian meteorites due to the

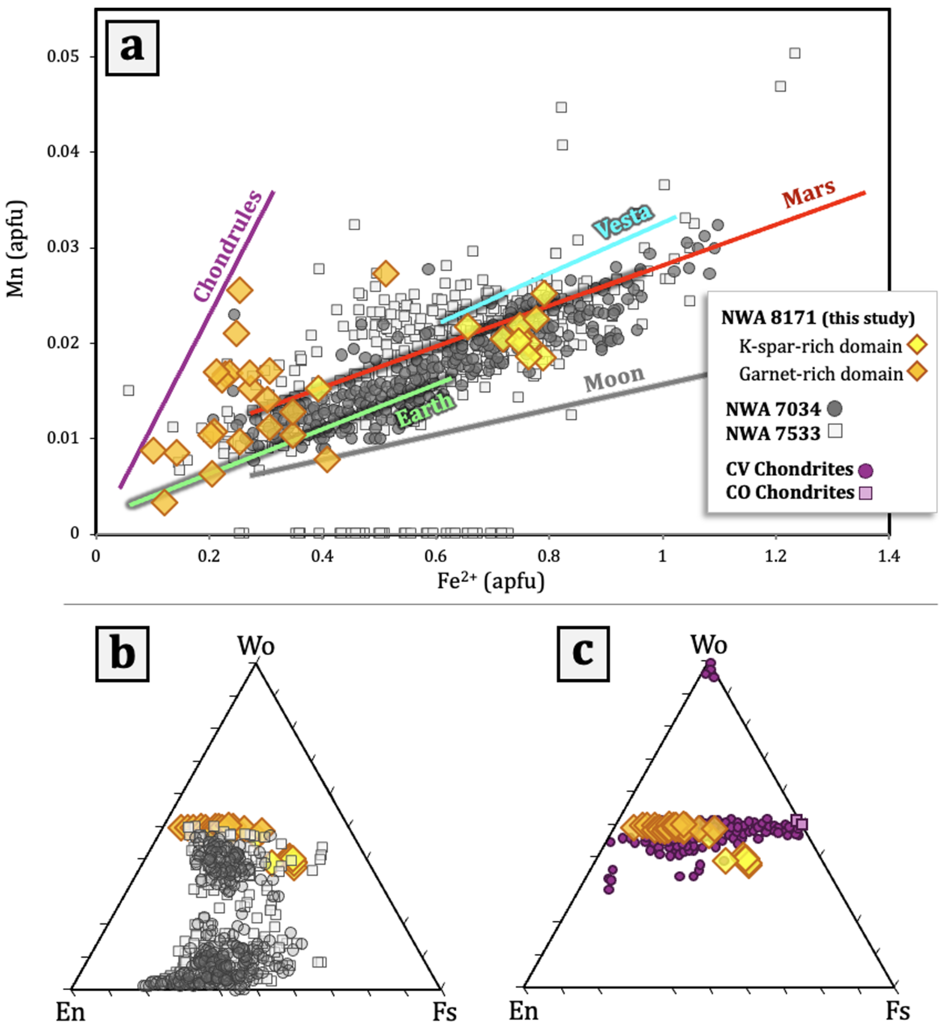

Figure 4 Comparisons between the garnet-bearing clast pyroxene compositions in NWA 8171 and other meteorites. **(a)** NWA 8171 pyroxene atoms *per* formula unit (apfu; based on 6 O) Mn and Fe^{2+} compositions in comparison to pyroxenes in paired martian breccias NWA 7034 and NWA 7533 (data points drawn after Agee *et al.*, 2013, and calculated from Hewins *et al.*, 2017, data; respectively), and other planetary bodies (achondrite trendlines after Papike *et al.*, 2009; chondrules trendline after Papike, 1998). **(b)** Major element pyroxenes comparisons between NWA 8171, martian regolith breccia pairs NWA 7034 and NWA 7533, and **(c)** CV and CO chondrites (data points after Ganino and Libourel, 2020 and references therein). Wo = molar $CaO/(CaO+MgO+FeO_T)$, En = molar $MgO/(CaO+MgO+FeO_T)$, Fs = molar $FeO_T/(CaO+MgO+FeO_T)$.

presence of maghemite and goethite (Gattacceca *et al.*, 2014). Mn oxides in paired breccia meteorites are also interpreted to have formed in ancient, long term oxidising aqueous environments on Mars (Liu *et al.*, 2021), and orbiters and *in situ* analyses have identified numerous oxidized phases on the martian surface (*i.e.* Morris *et al.*, 2006; Bibring *et al.*, 2006).

Regardless, it is still unclear if the chemistry and textures of the garnet-bearing assemblage represent the conditions at the time of formation, or after shock metamorphism. Given that the clast has been subjected to at least two shock metamorphism events (the breccia forming event, and ejection from Mars), and all major phases show evidence of deformation (Figs. 2, S-13), it is difficult to definitively determine which chemical and structural features retain their original signatures.

Further analyses will be needed to narrow down the origin and implications of the garnet-bearing clast. While destructive analyses have been avoided here due to the rarity of the clast, oxygen isotope measurements will likely be needed to definitively confirm its potential martian origin. However, if martian, the chemical and mineralogical details reported here indicate that the lithological diversity on Mars may be greater than previously assumed. If the andradite-bearing clast is a product of martian metasomatic or metamorphic processes, the clast could record the environmental conditions of ancient hydrothermal systems associated with impacts or intruding plutons (McSween *et al.*, 2015). Alternatively, if it formed at high temperatures, the clast may represent a previously unsampled source or differentiation pathway, potentially providing new insights into Mars' crustal evolution.

Acknowledgments

TVK was partially supported by the Dorothy Killam Fellowship awarded to KT. KT was supported by NSERC Discovery Grant 2022-04381. AČ acknowledges Rita Levi Montalcini fellowship (Italian MUR). Analyses at University of Portsmouth were supported by STFC grant ST/S000291/1 to JRD. Joe Dunlop and Geoff Long are thanked for their help collecting EBSD datasets. Yanan Liu and Brian Joy are thanked for helping collect microprobe maps and point measurements. The Mars image in the background of the graphical abstract is credited to JPL-NASA. We are grateful to Dr. Robert Hazen and one anonymous reviewer whose suggestions greatly improved this manuscript. We also thank Dr. Ambre Luguet for editorial handling and guidance.

Editor: Ambre Luguet

Declaration of AI Use

During the preparation of this work the author used OpenAI software for grammatical improvements while writing. The author reviewed and edited the resulting minor wording suggestions and takes full responsibility for the content of the publication. No interpretations, figures, or analyses were completed with AI.

Additional Information

Supplementary Information accompanies this letter at https://www.geochemicalperspectivesletters.org/article2619.

Cite this letter as: Kizovski, T.V., White, L.F., Černok, A., Tait, K.T., Di Cecco, V.E., Chu, X., Tomacic, J.M., Nicklin, R.I., Darling, J.R. (2026) Expanding Mars' lithologic diversity: discovery of a garnet-bearing clast in NWA 8171. *Geochem. Persp. Let.* 40, 30–37. https://doi.org/10.7185/geochemlet.2619

References

Agee, C.B., Wilson, N.V., McCubbin, F.M., Ziegler, K., Polyak, V.J., *et al.* (2013) Unique Meteorite from Early Amazonian Mars: Water-Rich Basaltic Breccia Northwest Africa 7034. *Science* 339, 780–785. https://doi.org/10.1126/science.1228858

Baxter, E.F., Caddick, M.J., Dragovic, B. (2017) Garnet: A Rock-Forming Mineral Petrochronometer. *Reviews in Mineralogy and Geochemistry* 83, 469–533. https://doi.org/10.2138/rmg.2017.83.15

Benisek, A., Kroll, H., Cemič, L. (2004) New developments in two-feldspar thermometry. *American Mineralogist* 89, 1496–1504. https://doi.org/10.2138/am-2004-1018

Bibring, J.-P., Langevin, Y., Mustard, J.F., Poulet, F., Arvidson, R., *et al.* (2006) Global Mineralogical and Aqueous Mars History Derived from OMEGA/Mars Express Data. *Science* 312, 400–404. https://doi.org/10.1126/science.1122659

Carter, J., Poulet, F., Bibring, J.-P., Mangold, N., Murchie, S. (2013) Hydrous minerals on Mars as seen by the CRISM and OMEGA imaging spectrometers: Updated global view. *Journal of Geophysical Research: Planets* 118, 831–858. https://doi.org/10.1029/2012JE004145

Chiama, K., Gabor, M., Lupini, I., Rutledge, R., Nord, J.A., *et al.* (2023) The secret life of garnets: a comprehensive, standardized dataset of garnet geochemical analyses integrating localities and petrogenesis. *Earth System Science Data* 15, 4235–4259. https://doi.org/10.5194/essd-15-4235-2023

Ehlmann, B.L., Mustard, J.F., Clark, R.N., Swayze, G.A., Murchie, S.L. (2011) Evidence for Low-Grade Metamorphism, Hydrothermal Alteration, and Diagenesis on Mars from Phyllosilicate Mineral Assemblages. *Clays and Clay Minerals* 59, 359–377. https://doi.org/10.1346/CCMN.2011.0590402

Ganino, C., Libourel, G. (2020) Fumarolic-like activity on carbonaceous chondrite parent body. *Science Advances* 6, eabb1166. https://doi.org/10.1126/sciadv.abb1166

Gattacceca, J., Rochette, P., Scorzelli, R.B., Munayco, P., Agee, C., *et al.* (2014) Martian meteorites and Martian magnetic anomalies: A new perspective from NWA 7034. *Geophysical Research Letters* 41, 4859–4864. https://doi.org/10.1002/2014GL060464

Hazen, R.M., Papineau, D., Bleeker, W., Downs, R.T., Ferry, J.M., McCoy, T.J., Sverjensky, D.A., Yang, H. (2008) Mineral evolution. *American Mineralogist* 93, 1693–1720. https://doi.org/10.2138/am.2008.2955

Hazen, R.M., Downs, R.T., Morrison, S.M., Tutolo, B.M., Blake, D.F., *et al.* (2023) On the Diversity and Formation Modes of Martian Minerals. *Journal of Geophysical Research: Planets* 128, e2023JE007865. https://doi.org/10.1029/2023JE007865

Hewins, R.H., Zanda, B., Humayun, M., Nemchin, A., Lorand, J.-P., *et al.* (2017) Regolith breccia Northwest Africa 7533: Mineralogy and petrology with implications for early Mars. *Meteoritics & Planetary Science* 52, 89–124. https://doi.org/10.1111/maps.12740

Humayun, M., Nemchin, A., Zanda, B., Hewins, R.H., Grange, M., *et al.* (2013) Origin and age of the earliest Martian crust from meteorite NWA 7533. *Nature* 503, 513–516. https://doi.org/10.1038/nature12764

Jenkins, L.E., Lee, M.R., Daly, L., King, A.J., Chung, P., *et al.* (2025) Identification of hydroandradite in CM carbonaceous chondrites: A product of calc-silicate alteration on C-complex asteroids. *American Mineralogist* 110, 1238–1248. https://doi.org/10.2138/am-2024-9389

Krot, A.N., Petaev, M.I., Scott, E.R.D., Choi, B.-G., Zolensky, M.E., Keil, K. (1998a) Progressive alteration in CV3 chondrites: More evidence for asteroidal alteration. *Meteoritics & Planetary Science* 33, 1065–1085. https://doi.org/10.1111/j.1945-5100.1998.tb01713.x

Krot, A.N., Petaev, M.I., Zolensky, M.E., Keil, K., Scott, E.R.D., Nakamura, K. (1998b) Secondary calcium-iron-rich minerals in the Bali-like and Allende-like oxidized CV3 chondrites and Allende dark inclusions. *Meteoritics & Planetary Science* 33, 623–645. https://doi.org/10.1111/j.1945-5100.1998.tb01668.x

Lafuente, B., Downs, R.T., Yang, H., Stone, N. (2016) 1. The power of databases: The RRUFF project. In: Armbruster, T., Danisi, R.M. (Eds.) *Highlights in Mineralogical Crystallography*. De Gruyter, Berlin, 1–30. https://doi.org/10.1515/9783110417104-003

Li, X.-P., Rahn, M., Bucher, K. (2004) Metamorphic Processes in Rodingites of the Zermatt-Saas Ophiolites. *International Geology Review* 46, 28–51. https://doi.org/10.2747/0020-6814.46.1.28

Liu, Y., Fischer, W.W., Ma, C., Beckett, J.R., Tschauner, O., *et al.* (2021) Manganese oxides in Martian meteorites Northwest Africa (NWA) 7034 and 7533. *Icarus* 364, 114471. https://doi.org/10.1016/j.icarus.2021.114471

MacPherson, G.J., Krot, A.N. (2014) The formation of Ca-, Fe-rich silicates in reduced and oxidized CV chondrites: The roles of impact-modified porosity and permeability, and heterogeneous distribution of water ices. *Meteoritics & Planetary Science* 49, 1250–1270. https://doi.org/10.1111/maps.12316

Malarewicz, V., Beyssac, O., Zanda, B., Marin-Carbonne, J., Leroux, H., *et al.* (2025) Evidence for pre-Noachian granitic rocks on Mars from quartz in meteorite NWA 7533. *Nature Geoscience* 18, 207–212. https://doi.org/10.1038/s41561-025-01653-z

McCubbin, F.M., Boyce, J.W., Novák-Szabó, T., Santos, A.R., Tartèse, R., *et al.* (2016) Geologic history of Martian regolith breccia Northwest Africa 7034: Evidence for hydrothermal activity and lithologic diversity in the Martian crust. *Journal of Geophysical Research: Planets* 121, 2120–2149. https://doi.org/10.1002/2016JE005143

McSween, H.Y. (2015) Petrology on Mars. *American Mineralogist* 100, 2380–2395. https://doi.org/10.2138/am-2015-5257

McSween, H.Y., Labotka, T.C., Viviano-Beck, C.E. (2015) Metamorphism in the Martian crust. *Meteoritics & Planetary Science* 50, 590–603. https://doi.org/10.1111/maps.12330

Morris, R.V., Klingelhöfer, G., Schröder, C., Rodionov, D.S., Yen, A., *et al.* (2006) Mössbauer mineralogy of rock, soil, and dust at Gusev crater, Mars: Spirit's journey through weakly altered olivine basalt on the plains and pervasively altered basalt in the Columbia Hills. *Journal of Geophysical Research: Planets* 111, E02S13. https://doi.org/10.1029/2005JE002584

Papike, J.J. (1998) *Planetary materials*. De Gruyter, Berlin. https://doi.org/10.1515/9781501508806

Papike, J.J., Karner, J.M., Shearer, C.K., Burger, P.V. (2009) Silicate mineralogy of martian meteorites. *Geochimica et Cosmochimica Acta* 73, 7443–7485. https://doi.org/10.1016/j.gca.2009.09.008

Payré, V., Udry, A., Fraeman, A.A. (2024) Igneous Diversity of the Early Martian Crust. *Minerals* 14, 452. https://doi.org/10.3390/min14050452

Schmidt, M.E., Kizovski, T.V., Liu, Y., Hernandez-Montenegro, J.D., Tice, M.M., *et al.* (2025) Diverse and highly differentiated lava suite in Jezero crater, Mars: Constraints on intracrustal magmatism revealed by Mars 2020 PIXL. *Science Advances* 11, eadr2613. https://doi.org/10.1126/sciadv.adr2613

Stormer, J.C., Pierson, M.L., Tacker, R.C. (1993) Variation of F and Cl X-ray intensity due to anisotropic diffusion in apatite during electron microprobe analysis. *American Mineralogist* 78, 641–648. http://www.minsocam.org/ammin/AM78/AM78_641.pdf

Tosca, N.J., Tice, M.M., Hurowitz, J.A., Pedersen, D.A.K., Henneke, J., *et al*. (2025) In situ evidence for serpentinization within the Máaz formation, Jezero crater, Mars. *Science Advances* 11, eadr8793. https://doi.org/10.1126/sciadv.adr8793

Udry, A., Howarth, G.H., Herd, C.D.K., Day, J.M.D., Lapen, T.J., Filiberto, J. (2020) What Martian Meteorites Reveal About the Interior and Surface of Mars. *Journal of Geophysical Research: Planets* 125, e2020JE006523. https://doi.org/10.1029/2020JE006523

Yen, A.S., Clark, B.C., Ming, D.W., Mittlefehldt, D.W., Gellert, R., Morris, R.V. (2010) Chemical Alteration on Mars Indicated by the Iron-Manganese Ratio. *41st Lunar and Planetary Science Conference*, abstract 2546. https://www.lpi.usra.edu/meetings/lpsc2010/pdf/2546.pdf